Investigation on the Melt Spinning Fibers of PP/Organoclay Nanocomposites Prepared by *In-Situ* Polymerization

Chaowei Hao,[1,2] Ying Zhao,[1] Aihua He,[1] Xiuqin Zhang,[1] Dujin Wang,[1] Qingfang Ma,[2] Yizhuang Xu[3]

[1]*Beijing National Laboratory for Molecular Sciences, CAS Key Laboratory of Engneering Plastics, Joint Laboratory of Polymer Science and Materials, Institute of Chemistry, Chinese Academy of Sciences, Beijing 100190, People's Republic of China*
[2]*Key Lab of Organosilicon Chemistry and Material Technology Ministry of Education, Hangzhou Normal University, Hangzhou 310012, People's Republic of China*
[3]*State Key Laboratory of Rare Earth Materials Chemistry and Applications, College of Chemistry and Molecular Engineering, Peking University, Beijing 100871, People's Republic of China*

Received 16 September 2008; accepted 8 March 2009
DOI 10.1002/app.30392
Published online 4 January 2010 in Wiley InterScience (www.interscience.wiley.com).

ABSTRACT: Fibers prepared by melt spinning process from the PP (polypropylene)/organoclay nanocomposite were characterized in details with the aid of SEM, FTIR, XRD, DSC, and mechanical measurements. The results suggested that the lower content of organoclay (0.1%) added to the PP matrix increased the crystallinity and mechanical property (tensile strength) of the PP/organoclay nanocomposite fiber. With increasing the content of organoclay ($\geq$ 0.3%), the crystallinity and the tensile strength both a little decreased, and the fiber containing organoclay exhibited multi-peaks at the same draw ratio during the heating process. Furthermore, the degree of orientation of the fiber increased a little with lower content of organoclay (0.1%) introduction to PP during the infrared dichroism measurement. © 2010 Wiley Periodicals, Inc. J Appl Polym Sci 116: 1384–1391, 2010

Key words: fibers; nanocomposites; *in-situ* polymerization; orientation; PP

INTRODUCTION

Recently, polymer nanocomposites rooted in the incorporation of organic or inorganic filler attracted considerable attention from researchers all over the world because of the promising improvement in the mechanical and dimensional stability, stiffness, and impact resistance or decrease flammability as well in contrast with that of the polymer matrix.[1–10] Depending on the strength of interfacial interactions between the polymer matrix and layered silicate (modified or not), three different types of PLS nanocomposites are thermodynamically achievable, intercalated nanocomposites, flocculated nanocomposites, and exfoliated nanocomposites.

Polymer fibers are commonly applied as textiles, carpets, or as additives to reinforce material properties.[11–13] Up to now, despite successful attempts to transfer carbon nanofiber and montmorillonite-modified polymer nanocomposites into fiber,[14–28] difficulties result from particle aggregation, from polymer degradation catalyzed by the additives, resulting in brittle fibers. Haider recently reported that multiwalled carbon nanotube/nylon-6 nanocomposites (MWNT/nylon-6) were prepared by *in situ* polymerization,[26] and obtained fibers by electrospinning. But for nonpolar polymer, as for PP, the homogeneous good processability during the preparation and drawing of composite fibers requires a homogeneous distribution of the filler in the polymer matrix.

This study is a continuation of our previous basic study of a series of polypropylene (PP) nanocomposites,[24,25] which were successfully prepared by directly melting intercalative blended of PP with nanoparticles. Tudor et al.[29] first used the *in-situ* intercalative polymerization method for the preparation of PP/clay nanocomposites. Unfortunately, the authors did not report any characterization of these composites. In another recent publication, Sun and Garces[30] reported the preparation of PPCNs by *in-situ* intercalative polymerization with metallocene/clay catalysts. But up to present, there has no publication discussing the spinning of the PP/clay

Correspondence to: Y. Zhao (yzhao@iccas.ac.cn).
Contract grant sponsor: 973 Program of the Ministry of Science and Technology; contract grant number: 2003CB615600.
Contract grant sponsor: attracting high-quality personnel program of the Hangzhou Normal University; contract grant number: D04193001.

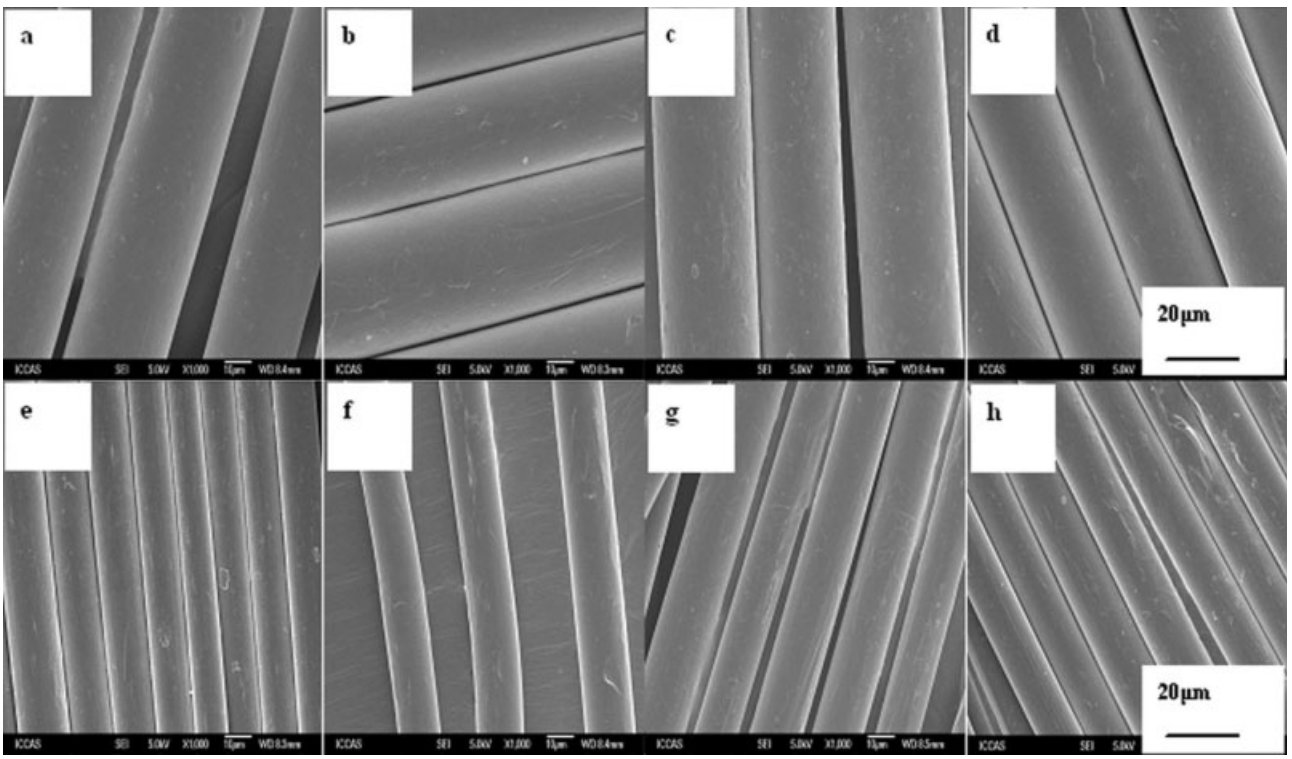

Figure 1 The SEM pictures of the PP and nanocomposite fibers. (a–d): The as-spun fibers, (a) PP; (b–d) 0.1, 0.3, and 0.5% organoclay, respectively; (e–h) fibers with draw ratio 4, (e) PP; (f–h) 0.1, 0.3, and 0.5% organoclay, respectively.

nanocomposites prepared by *in-situ* intercalative polymerization. Considering the poor dispersibility of organoclay in PP matrix by direct melt intercalative blending, here, the uniformly dispersed anisotropic nanoparticle was achieved by preparing PP/organoclay nanocomposites by *in-situ* polymerization of PP with silicate nanoparticles. And in this work, the influence of organoclay and the spinning process on the properties and morphology of the PP nanocomposite fibers are observed.

EXPERIMENTAL

Materials and preparation of PP/organoclay nanocomposites

The nanocomposites consisted of PP with a melt flow index (MFI) of 7.40 g/10 min, which was synthesized in kettle and the organophilic silicate filler that was added to the kettle before the polymeric reaction beginning. And the cation-exchange capacity value of the Na^+-based montmorillonite is 90–100 mmol/100 g.

Spinning conditions for nanocomposite fibers

The composite fibers containing 0.1, 0.3, and 0.5% of organoclay was prepared from granulated polymer with a laboratory single-screw ($L/D = 25$) melt extruder with a spinneret containing 48 orifices, each 0.35 mm in diameter. The extruder was set with temperature zone of 200, 220, 230, 225, and 200°C at the feed, metering, melt-blending, die, and spinneret sections, respectively. And the as-spun filaments were collected at a take-up speed of 500 m/min and drawn at 100°C on a four-positioned drawing platform with the draw ratio being 2, 3, 3.5, and 4, respectively.

Characterization of nanocomposits fibers

Morphology

The scanning electron microscopy (SEM) images were taken from fiber surfaces with a Hitachi S 4300 SEM with platinum sputtering.

Infrared dichroism and X-ray analysis of PP and PP/organoclay nanocomposites fibers

The degree of fiber orientation was measured by polarized infrared spectroscopy method with a Bruker EQUINOX 55 spectrometer. The parallel and perpendicular spectra were collected by averaging 32 scans at a 4 cm^{-1} resolution.

To measure the crystallinity and the grain size of PP and PP/organoclay hybrid fibers, XRD data between 5 and 35° were collected by using a Rigaku D/MAX-RB X-ray diffractometer with CuK radiation

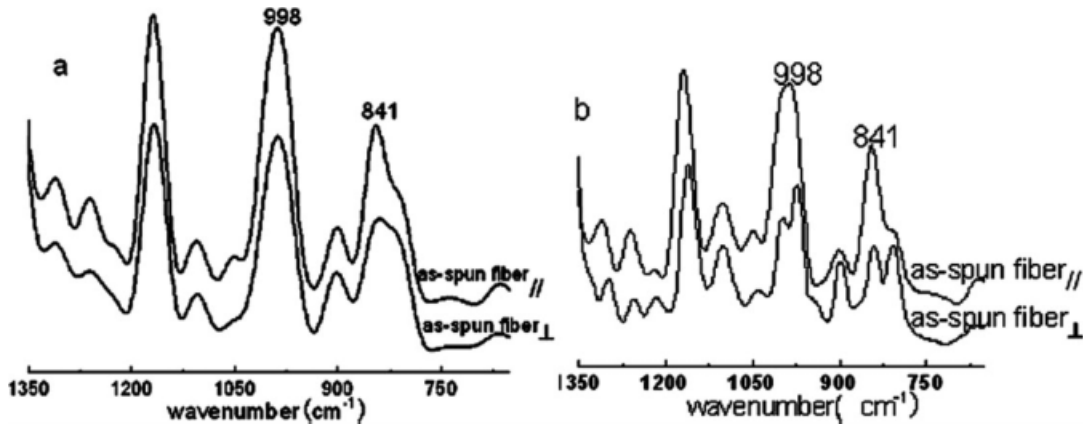

Figure 2 (a) The infrared dichroism result of the as-spun fiber for pure PP; (b) The infrared dichroism result of the as-spun fiber for PP containing 0.5% organoclay.

at a generator voltage of 40 kV and a generator current of 50 mA.

Differential scanning calorimetry

DSC measurements were performed at a Perkin-Elmer DSC-7 to determine the crystallinity of the polypropylene from the endothermic melting process.[31] Samples were treated with the following procedure. Samples were hold for 1 min at 40°C and heated from 40 to 230°C at 10°C/min, then held for 5 min followed by the cooling process from 230 to 40°C at 10°C /min. The enthalpy of fusion (H_f) was calculated by dividing the endothermic peak area by the weight of polypropylene within the composite sample. Crystallinities (X_c) of the different composites were obtained by dividing H_f by the extrapolated value of enthalpy corresponding to the melting of 100% crystalline PP of $H_f^0 = 170\,\mathrm{J/g}$.[32]

Mechanical measurements

Mechanical measurements of the fibers were performed with an IX automated materials testing system from Instron Corp. The stress was measured as a function of the elongation of a bundle of 48 fibers at an initial length of 10 cm. Elongation was increased at a velocity of 100 mm/min for the drawn ones. From these stress elongation measurements, the maximum stress per area (cN/dtex), and the elongation at break were determined. All samples were measured five times, and the results were averaged to obtain a mean value.

RESULTS AND DISCUSSION

Morphology of PP and nanocomposite fibers

The morphology of the PP nanocomposite fibers was observed using SEM. The micrographs in Figure 1 displayed the difference of the surface of PP and nanocomposite fibers. The surface of PP fibers was smooth and plain, whereas for PP/organoclay nanocomposite fibers, the surface had many flaws and grooves for both the as-spun and drawn fibers. Furthermore, with increasing the content of organoclay in nanocomposite fibers, the surface coarseness of the fibers became larger, which suggests the organoclay had some effects on the morphology of the fibers. In other words, the organoclay had influenced the morphology formation during the spinning process, which implied that the properties of the nanocomposites' fibers, such as the mechanical and thermal properties, might be influenced by the added organoclay.

TABLE I
The Orientation Degree of PP and Nanocomposite Fibers with Changing Draw Ratio Based on the FTIR Results

Draw ratio / Orientation degree of fibers	1	2	4
Pure PP	0.14	0.23	0.34
PP containing 0.1% organoclay	0.20	0.24	0.35
PP containing 0.5% organoclay	0.13	0.23	0.33

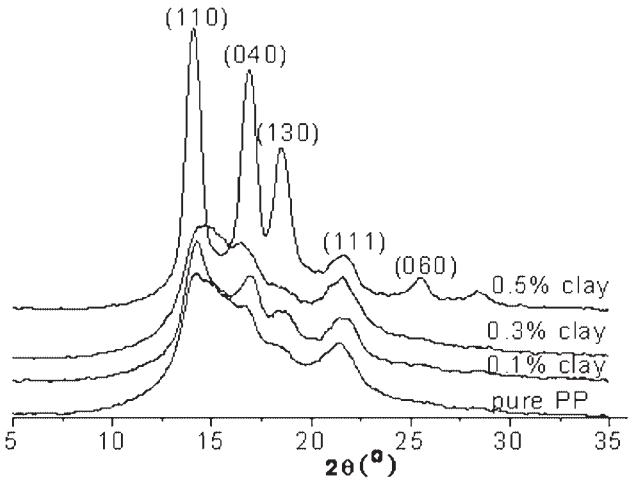

Figure 3 XRD results of the as-spun fibers with the variation of the ogranoclay content.

Infrared dichroism and X-ray analysis

The orientation of the PP and nanocomposite fibers was calculated by polarized infrared spectroscopy. The specific formulas are follows:

$$R = A_{\parallel}/A_{\perp} \tag{1}$$

Where $A_{\parallel}$ and $A_{\perp}$ are the absorption intensity of the paralleling and verticalizing direct of the incident ray, respectively, and the R is dichroic ratio, which means the ratio of $A_{\parallel}$ to $A_{\perp}$.

The average orientation in crystal zone, f_c, of the fibers are expressed by f_{c1} and f_{c2},[33] where,

$$f_{c1} = [2/(3\cos^2 18^\circ - 1)]^*[(R_{998} - 1)/(R_{998} + 2)] = 1.167^*[(R_{998} - 1)/(R_{998} + 2)] \tag{2}$$

$$f_{c2} = [(R_{841} - 1)/(R_{841} + 2)] \tag{3}$$

$$f_c = (f_{c1} + f_{c2})/2 \tag{4}$$

Based on the above formulas, the orientation of the fiber was calculated, as was shown in Figure 2 and Table I. The results show that the orientation of both PP and nanocomposite fibers increase with the draw ratio increasing. And the orientation of nanocomposite fibers is nearly the same with that of the pure PP fiber at the same draw ratio, which addressed that the organoclay has no much influence on the orientation of fibers within the given range of the organoclay content.

Generally, iPP is a multicrystalline polymer and has five crystalline forms (i.e., α, β, γ, δ, and pseudohexagonal, etc.). The XRD study shows that the containing organoclay clearly affects the crystalline form of as-spun fibers (Fig. 3). The different diffraction peaks were exhibited from the XRD curves of the PP and nanocomposite fibers containing higher organoclay content. The pure PP fibers shows two major peaks, located at $2\theta = 15.0^\circ$ and 21.5°, which correspond to the pseudohexagonal crystalline diffraction peaks, whereas nanocomposite as-spun fibers containing 0.5% organoclay content exhibits distinct α-crystalline diffraction peaks at $2\theta = 14.1^\circ$, 16.8°, 18.5°, 21.5°, and 25.5°, which is often produced under more efficient crystallization conditions, e.g. drawing and annealing, etc. The XRD results might imply that the nanocomposite as-spun fibers crystallized much faster than that of the pure PP as-spun fiber, which might be reflected by the crystallinity of the fibers. And from Figure 4, it was found that the α-crysatlline form dominated for all the drawn fibers (including the pure PP and nanocomposite fibers), meaning that the organoclay has no clearly effect on the crystal forms of the drawn PP fibers. In addition, the crystallinity of the PP and nanocomposite fibers were calculated by the curve fitting of the XRD curves correspondingly. Figure 5 shows the curve fitting results of the pure PP and nanocomposite fibers with the draw ratio being 4, which could be

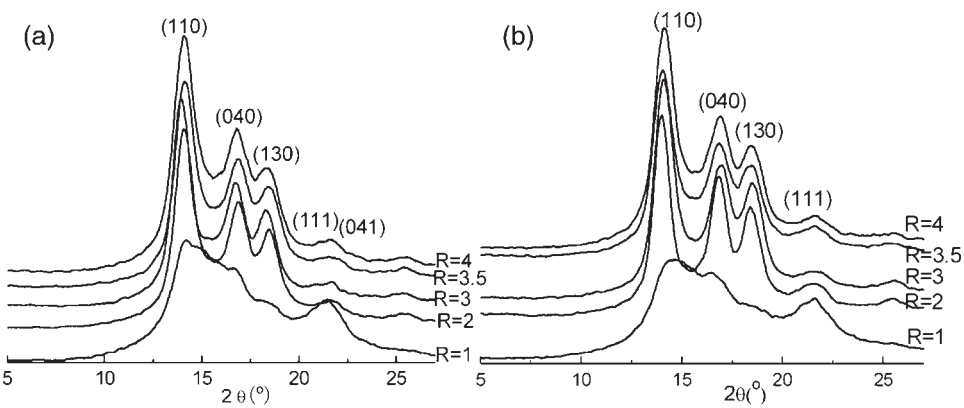

Figure 4 (a) The XRD results of the fibers with the variation of the draw ratio for pure PP; (b) The XRD results of the fibers with the variation of the draw ratio for PP containing 0.3% organoclay.

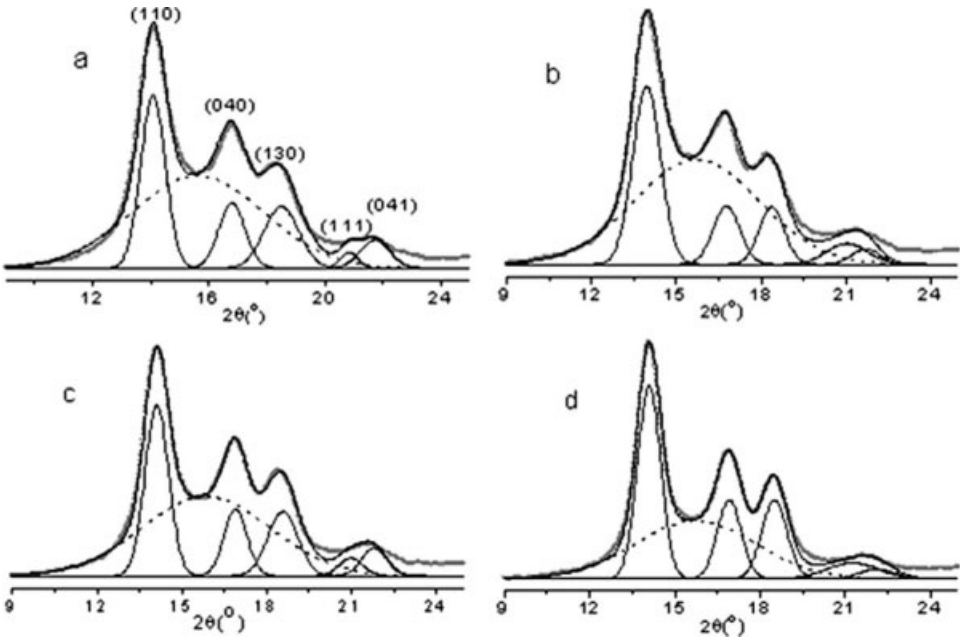

Figure 5 (a) Curve fitting XRD results of the fibers with the draw ratio 4 for pure PP; (b) Curve fitting XRD results of the fibers with the draw ratio 4 for PP containing 0.1% organoclay; (c) Curve fitting XRD results of the fibers with the draw ratio 4 for PP containing 0.3% organoclay; (d) Curve fitting XRD results of the fibers with the draw ratio 4 for PP containing 0.5% organoclay.

found that the integrated area of the amorphous domains decreased with the introduction of the organoclay into PP. And the integrated area also decreased with increasing the organoclay content, which indicated that the crystallinity of nanocomposite fibers was improved. The specific crystallinity of the pure PP and nanocomposite fibers was calculated based on the following formula,[34]

$$X_c = I_c/(I_c + I_a) * 100\% \quad (5)$$

where I_c and I_a are the integrated areas of the crystalline and amorphous domains, respectively, and X_c is the average crystallinity of the system. The data shown in Table II shows that the crystallinity of the drawn fibers increases with increasing the organoclay content and is higher than that of the pure PP fiber, which suggests again that certain organoclay added to the PP fibers could act as the nucleating agent and promote the crystal growth of the PP crystal in an essential way and perfected the α-crystalline form.

TABLE II
The Crystalinity of PP and Nanocomposite Fibers with Changing Organoclay Content Based on the XRD and DSC Results

Draw ratio					
Crystallinity	1	2	3	4	4 (XRD)
Pure PP (%)	45.5	52.8	56.6	57.5	43.2
0.1% clay (%)	48.6	53.7	57.5	59.6	44.2
0.3% clay (%)	45.1	53.0	55.7	57.4	45.9
0.5% clay (%)	45.6	52.7	55.4	57.0	47.8

Differential scanning calorimetry for the fibers

Figure 6 shows the melting and crystallization behaviors of the as-spun fibers with increasing the organoclay content. It was shown that the organoclay affect both the melting and the crystallization temperatures. As shown in Figure 6(a), compared with the broad and sole endothermic peak of the pure PP as-spun fibers, the peaks of the nanocomposite fibers become narrow and exhibit a sub-peak with increasing the organoclay content, which indicated that there may exist different crystal forms or different thickness of the lamellar crystal, agreeing with the XRD results reflected in Figure 3.

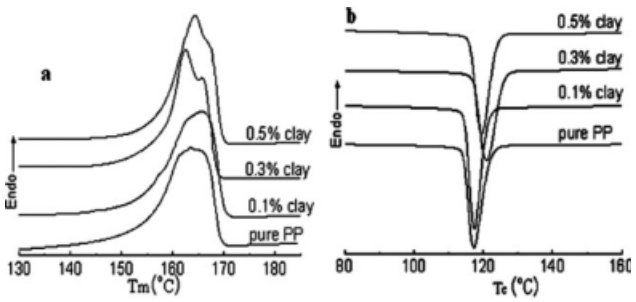

Figure 6 (a) The DSC results of PP and PP nanocomposite as-spun fibers during heating scan; (b) The DSC results of PP and nanocomposite as-spun fibers during cooling scan.

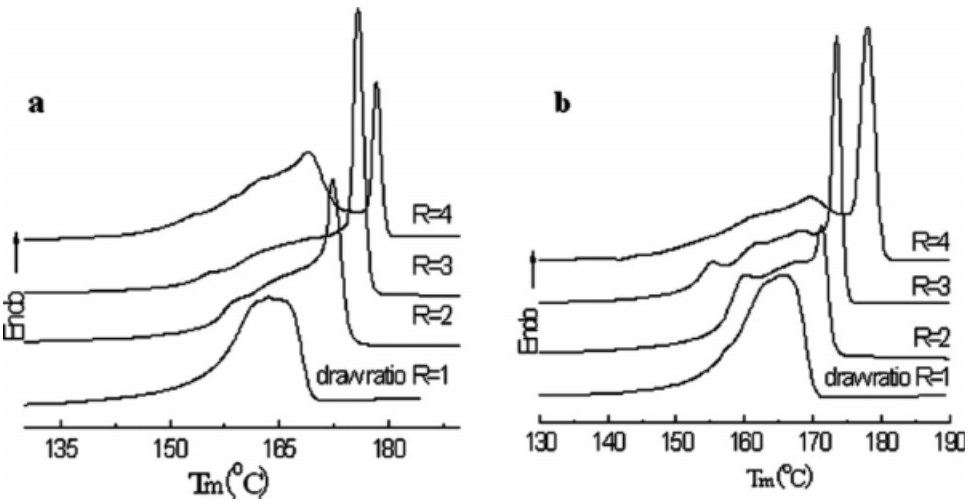

Figure 7 (a) The DSC results of pure PP fibers with changing the draw ratio; (b) The DSC results of PP nanocomposites fibers with changing the draw ratio.

Furthermore, as the aforementioned argument that the organoclay could act as the nucleating agent and accelerate the crystal growth of the PP fibers, the crystallization temperatures of the nanocomposite as-spun fibers were clearly enhanced compared with that of the pure PP as-spun fibers [Fig. 6(b)]. It is also evident that there is a distinct exothermic crystallization peak in all of the cooling scans, and the peak is symmetrical. And with increasing the organoclay content, the crystallization temperature of the as-spun nanocomposite fibers first increased and then decreased after experiencing a maximum value, which might be related to the influence of organoclay on the crystallization mechanism.

In programmed cooling, the crystallization temperature reflects the overall crystallization rate, attributed to the combined effects of nucleation and growth. It is known that the organoclay is an effective nucleating agent due to the high surface area of silicate platelets and their chemical affinity for the polymer, which induce a nucleation and lamellar ordering effect. When small quantity organoclay was added, the organolcay acts as nucleating agent and heightens the crystallization rate and induces the crystallization at higher temperature compared with that of the pure PP fibers. However, with the organoclay content further increasing, the organoclay begins to aggregate and could confine the mobility of the polymer chains to rearrangement and form crystal grains, which is to say, the higher content of the organoclay eased the crystal growth of the fibers and finally induced the decrease of the crystallization temperature of the nanocomposite fibers but is still higher than that of the pure PP fibers.

Figure 7 shows the melting behaviors of pure PP and nanocomposite drawn fibers with changing the draw ratio. It suggests that the endothermic peaks of all the drawn fibers moved to higher temperature with increasing the draw ratio. The melting temperature increasing with the increase of the draw ratio is ascribed to the increase of the orientation degree, crystallinity and the crystal perfectness of the fibers through the drawing process. And the variational trend of the melting temperatures of the nanocomposite drawn fibers with the draw ratio is similar with that of the pure PP drawn fibers, which again suggests that the organoclay has no obvious effect on the crystal forms of the drawn fibers, agreeing with the XRD results showed in Figure 4. And the crystallinity of the drawn fibers was calculated as well (Table II). The results show that the crystallinity of all the drawn fibers at lower draw ratio ($R \leq 3$) increased much with increasing the draw ratio, whereas for higher draw ratio (e.g., $R = 4$), the crystallinity of the fibers increased slightly. The reason is that the restriction on the stretched chains becomes greater and thus makes the chains more difficult to reconfigure into the correct helical registration that is necessary for crystallization.[35] Furthermore, the crystallinity of nanocomposite fibers containing lower organoclay content (e.g., 0.1%) is always larger than that of the pure PP fibers at the same draw ratio, which indicated that small amount of organoclay could clearly promote the crystal growth, agreeing with the FTIR result about the orientation degree of the fibers. And the result might suggest the better mechanical properties of the nanocomposite fibers at this nanoclay content.

Figure 8 shows the influence of organoclay content on the melting behavior of PP and nanocomposite fibers with draw ratio being 4. It can be seen that the organoclay content clearly affects the melting temperature of the drawn fiber. Compared with the endothermic peaks of the pure PP fibers, with lower

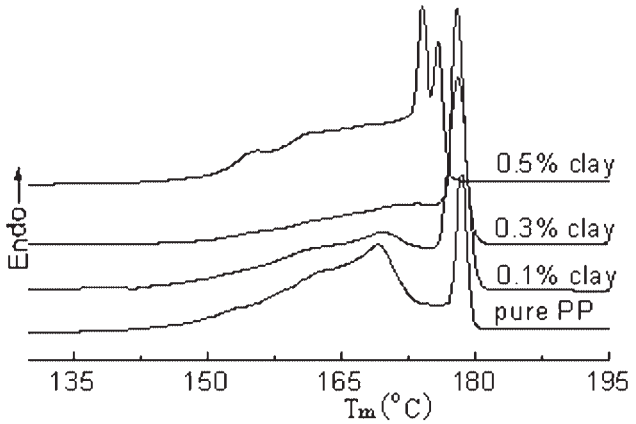

Figure 8 The influence of organoclay content on the melting behavior of PP and nanocomposite fibers (draw ratio = 4).

organoclay content addition to, the endothermic peak located at higher temperature of the fibers become sharper, accompanied by the peaks at lower temperature weakening, which indicates that the crystal phase of the fiber became more perfect in presence of a small quantity of organoclay. However with higher organolcay content introduction, the endothermic peaks become broad and move to lower temperature. When higher organoclay content was added, the clay may aggregate, confine the free molibity and crystallization of the chains and finally leads to the imperfect crystal producing, which induces the occurrence of the lower and broad endothermic peaks reflected on the heating curves. That is to say, the higher content of organoclay brings on the wider crystal distribution due to the cooperative effects of nucleation and restriction by the organoclay.

Mechanical measurement for fibers

Mechanical measurements of the fibers differed clearly upon variation of the organoclay content. And the measurements were performed on a bundle of 48 fibers of PP and nanocomposites with different organoclay content. Results on the elongation at maximum stress and the tensile strength of the fibers are shown in Table III. For the elongation at maximum stress, on the one hand, the values clearly decrease with the increase of the draw ratio for both the PP and the nanocomposites fibers, which could easily be understood by consideration about the orientation and crystallinity of the fibers increasing after drawing the fibers. On the other hand, the values about the elongation at maximum stress of the nanocomposite fibers are larger than that of the pure PP fibers and increased with the content of organoclay at the same draw ratio except that of the draw ratio 3. It was argued in DSC section that the fiber was inclined to deform due to the wider crystal distribution in the presence of organoclay, which accounts for the larger elongation at maximum stress than that of the pure PP fibers at the same draw ratio.

And for the tensile strength, the values obviously increase with increasing the draw ratio for both PP and the nanocomposites fibers, which also could easily be understood based on cognition about the orientation and crystallinity of fibers increasing. Whereas with increasing the organoclay content, the variation of the tensile strength values become complicated for the fibers at the same drawn ratio. With the introduction of a small quantity organoclay to PP matrix, e.g., 0.1% of organoclay content, the tensile strength of the fibers is clearly larger than that of the pure PP fibers in the drawn ratio 2, 3, 3.5, and 4. With continuing increase of the organoclay content, the values begin decreasing compared with that of the pure PP fibers, but the decreasing extent is small. Namely, small content of organoclay favors the increasing of the tensile strength of the fibers, whereas the higher organoclay content favors little decrease the tensile strength of the fibers. When small amount organoclay was added, the clay dispersed well in PP matrix and the PP molecular chains could tether on the clay slice or confine between the clay slices, which restricted the free

TABLE III
The Elongation at Maximum Stress (%) and the Tensile Strength (*cN*/*d*tex) of the PP and the Nanocomposites Fibers

Draw ratio / Samples	2	3	3.5	4
Elongation at maximum stress (%)				
Pure PP	86.7	40.1	17.9	15.1
PP with 0.1% caly	121.2	25.8	18.2	17.1
PP with 0.3% caly	141.8	29.0	19.6	18.4
PP with 0.5% caly	142.4	29.8	20.8	18.8
Tensile strength (*cN*/*d*tex)				
Pure PP	2.27	3.79	4.74	5.52
PP with 0.1% caly	2.83	4.06	4.97	6.36
PP with 0.3% caly	2.46	3.54	4.65	5.17
PP with 0.5% caly	2.29	3.31	4.37	4.67

mobility of the chains and induced the increase of the tensile strength of the fibers. With increasing the organoclay content, the clay could begin to aggregate, form the micro-phase separation structure and induce the focus of the stress during the drawing process, which finally result the small reduction of the tensile strength of the fibers. The results are well agreed with the FTIR, XRD, and DSC results aforementioned in this article. That is to say, the mechanical properties of the fibers are tightly related to the orientation degree, crystallinity, the crystal distribution, and the organoclay content in the composites.

CONCLUSIONS

PP/organoclay nanocomposites were prepared by *in-situ* intercalative polymerization and fibers were obtained from the nanocomposites by melt spinning process. FTIR and XRD analysis indicate that the orientation and crystallinity was influenced by the organoclay. DSC analysis showed that PP exhibited heterogeneous nucleation in the presence of organoclay and an increased crystallinity at lower organoclay content. Organoclay not only has effective nucleating effect, but also has the restricted effect clearly exhibited at higher organoclay content. The mechanical measurement suggested that the tensile strength and the elongation at maximum stress were both correlative with the organoclay content. It was concluded that the mechanical properties of the fibers are tightly related to the orientation degree, crystallinity, the crystal distribution, and the organoclay content in the composites.

References

1. Reichert, P.; Nitz, H.; Klinke, S.; Brandsch, R.; Thomann, R.; Mülhaupt, R. Macromol Mater Eng 2000, 275, 8.
2. Ke, Y.; Lü, J.; Yi, X.; Zhao, J.; Qi, Z. J Appl Polym Sci 2000, 78, 805.
3. Zanetti, M.; Camino, G.; Thomann, R.; Mülhaupt, R. Polymer 2001, 42, 4501.
4. Heinemann, J.; Reichert, P.; Thomann, R.; Mülhaupt, R. Macromol Rapid Commun 1999, 20, 423.
5. Dietsche, F.; Thomann, Y.; Thomann, R.; Mülhaupt, R. J Appl Polym Sci 2000, 75, 396.
6. Hasegawa, N.; Kawasumi, M.; Kato, M.; Usuki, A. J Appl Polym Sci 1998, 67, 87.
7. Zilg, C.; Thomann, R.; Mülhaupt, R.; Finter, J. Adv Mater 1999, 11, 49.
8. Giannelis, E. P. Adv Mater 1996, 8, 29.
9. Biswas, M.; Sinha, R.ayS. Adv Polym Sci 2001, 155, 167.
10. Ray, S. S.; Okamoto, M. Prog Polym Sci 2003, 28, 1539.
11. Schultze-Gebhardt, F.; Herlinger, K. H.Ullmann's Encyclopedia of Industrial Chemistry; Wiley-VCH: Weinheim, 2002; p 10.
12. Elias, H. G.An Introduction to Polymer Science; Wiley-VCH: Weinheim, 1997.
13. Stibal, W.; Schwarz, R.; Kemp, U.; Bender, K.; Weger, F.; Stein, M.Ullmann's Encyclopedia of Industrial Chemistry; Wiley-VCH: Weinheim, 2002; p 3.
14. Guan, G. H.; Li, C. C.; Zhang, D. J Appl Polym Sci 2005, 95, 1443.
15. Yoon, K. H.; Polk, M. B.; Min, B. G.; Schiraldi, D. A. Polym Int 2004, 53, 2072.
16. Chang, J. H.; Kim, S. J.; Im, S. Polymer 2004, 45, 5171.
17. Chang, J. H.; Kim, S. J.; Joo, Y. L.; Im, S. Polymer 2004, 45, 919.
18. Ergungor, Z.; Cakmak, M.; Batur, C. Macromol Symp 2002, 185, 259.
19. Ibanes, C.; David, L.; De Boissieu, M.; Seguela, R.; Epicier, T.; Robert, G. J Polym Sci Part B: Polym Phys 2004, 42, 3876.
20. Usuki, A.; Kato, M.; Okada, A.; Kurauchi, T. J Appl Polym Sci 1997, 63, 137.
21. Mlynarcikova, Z.; Borsig, E.; Legen, J.; Marcincin, A.; Alexy, P. J Macromol Sci Pure Appl Chem 2005, 42, 543.
22. Mlynarčíková, Z.; Kaempfer, D.; Thomann, R.; Mülhaupt, R.; Borsig, E.; Marcinčin, A. Polym Adv Technol 2005, 16, 362.
23. Paliková, S.; Thomann, R.; Reichert, P.; Mülhaupt, R.; Marcinčin, A.; Borsig, E. J Appl Polym Sci 2003, 89, 604.
24. Rottstegge, J.; Zhang, X. Q.; Zhou, Y.; Han, C. C.; Wang, D. J. J Appl Polym Sci 2007, 103, 218.
25. Zhang, X. Q.; Yang, M. S.; Zhao, Y.; Zhang, S. M.; Dong, X.; Liu, X. X.; Wang, D. J.; Xu, D. F. J Appl Polym Sci 2004, 92, 552.
26. Saeed, K.; Park, S. Y.; Haider, S.; Baek, J. B. Nanoscale Res Lett 2009, 4, 39.
27. Mun1, M. K.; Kim, J. C.; Chang, J. H. Polym Bull 2006, 57, 797.
28. Janowska, G.; Mikołajczyk, T.; Olejnik, M. J. Therm Anal Calorim 2008, 92, 495.
29. Tudor, J.; Willington, L.; O'hare, D.; Royan, B. Chem Commun 1996, 2031.
30. Sun, T.; Garces, J. M. Adv Mater 2002, 14, 128.
31. Boudenne, A.; Ibos, L.; Fois, M.; Gehin, E.; Majeste, J. C. J Polym Sci Part B: Polym Phys 2004, 42, 722.
32. Chan, C. M.; Wu, J.; Li, J. X.; Cheung, Y. K. Polymer 2002, 43, 2981.
33. Hobbs, J. P.; Sung, C. S. Macromolecules 1983, 16, 193.
34. Nurul Huda, M.; Dragun, H.; Bauer, S.; Muschik, H. Colloid Polym Sci 1985, 263, 730.
35. Ran, S. F.; Zong, X. H.; Fang, D. F.; Hsiao, B. S.; Chu, B. J. Macromolecules 2001, 82, 3172.